






## Optimized D- $\alpha$ -tocopherol polyethylene glycol succinate/phospholipid self-assembled mixed micelles: A promising lipid-based nanoplatform for augmenting the antifungal activity of fluconazole

SHAIMAA M. BADR-ELDIN<sup>1,2,\*</sup>   
HIBAH M. ALDAWSARI<sup>1,3</sup>  
USAMA A. FAHMY<sup>1,4</sup>  
OSAMA A. A. AHMED<sup>1,4</sup>  
NABIL A. ALHAKAMY<sup>1,3,4</sup>   
MAHMOUD A. ELFAKY<sup>5</sup>   
ALAA SIRWI<sup>5</sup>   
SALMAN A. HAWSAWI<sup>6</sup>  
ALI H. ALZAHIRANI<sup>6</sup>  
ABDULRAHMAN Y. YASEEN<sup>6</sup>  
MOHANNAD QASSIM<sup>6</sup>  
SABNA KOTTA<sup>1,3</sup> 

<sup>1</sup> Department of Pharmaceutics, Faculty of Pharmacy, King Abdulaziz University, Jeddah 21589, Saudi Arabia

<sup>2</sup> Department of Pharmaceutics and Industrial Pharmacy, Faculty of Pharmacy, Cairo University, Cairo, Egypt

<sup>3</sup> Center of Excellence for Drug Research and Pharmaceutical Industries, King Abdulaziz University, Jeddah 21589, Saudi Arabia

<sup>4</sup> Mohamed Saeed Tamer Chair for Pharmaceutical Industries, King Abdulaziz University, Jeddah 21589, Saudi Arabia

<sup>5</sup> Department of Natural Products, Faculty of Pharmacy, King Abdulaziz University, Jeddah 21589, Saudi Arabia

<sup>6</sup> Faculty of Pharmacy, King Abdulaziz University, Jeddah 21589, Saudi Arabia

Accepted December 27, 2021  
Published online December 27, 2021

### ABSTRACT

Fluconazole (FLZ) is the most widely used antifungal agent for treating cutaneous candidiasis. Although oral FLZ has been proved to be effective, the incidence of side effects necessitates the development of an effective formulation that could surpass the pitfalls associated with systemic availability. Accordingly, this research aimed at developing a self-assembled mixed micelles topical delivery system to enhance the topical delivery of the drug. Self-assembled mixed micelles were developed using D- $\alpha$ -tocopheryl polyethylene glycol 1000 succinate and phospholipids and optimized using Box-Behnken design. The optimized formulation with minimized size was then tested *in vivo* for the antifungal activity against *C. albicans* in immunocompromised mice. Treatment with the optimized formulation led to decreased peripheral erythema as well as lesions due to fungal infection in comparison to raw FLZ loaded gel. Therefore, the developed formulation was found to be a promising vehicle for the treatment of cutaneous candidiasis.

**Keywords:** fluconazole, fungal infections, *Candida albicans*, self-assembled mixed micelles, D- $\alpha$ -tocopheryl polyethylene glycol 1000 succinate, phospholipids

Fungal infections prevalence has increased worldwide by virtue of several causative factors including utilization of broad-spectrum antibiotics and elevated numbers of immune-compromised people (1). These factors can lead to the changing of commensal fungal species to pathogenic ones, thereby leading to the spread of fungal diseases

\* Correspondence; e-mail: smbali@kau.edu.sa

especially in susceptible individuals (2). Fungal infections range from superficial ones affecting the skin to systemic ones invading the body's interior. Cutaneous candidiasis is a common superficial skin infection caused by various *Candida* species, mostly *Candida albicans* (*C. albicans*). The clinical manifestations of such infection include dry, erythematous, or flaky skin (3). Azoles are the most commonly used antifungal drugs for the treatment and prevention of candidiasis (4), whereas fluconazole (FLZ) is the most widely used triazole with proven efficacy against the majority of pathogenic fungi and some Gram-positive bacteria (5). Oral FLZ has been proved to be effective against candidiasis at once-weekly oral doses of 150 mg (6). Despite the good tolerance and the low toxicity risk associated with FLZ oral administration, adverse reactions including gastrointestinal irritation, taste disorders, hepatotoxicity especially in immune-compromised subjects, in addition to anaphylactic and allergic responses have been reported (7). The possibility of occurrence of such side effects necessitates the development of an effective FLZ formulation that could surpass the systemic availability of the drug. Thereby, researchers have attempted to develop topical FLZ formulations including microemulsions, hydrogels, lipidic nanoparticles, liposomes, and cubosomes (8–10).

Researches in the drug formulation arena have recently focused on nanotechnology applications (11). Amongst the nanocarriers investigated, micelles have attracted attention for enhancing the delivery of drugs via the diversity of routes (12, 13). Micelles, developed by the self-assembly of amphiphilic molecules, are regarded as efficacious drug carriers due to their miniature size and solubilizing capability for poorly soluble drugs (14). Self-assembled mixed micelles (SAMMs), developed using two or more amphiphilic molecules, allow for the simultaneous incorporation of multiple functionalities into one formulation (15). SAMMs provide additional advantages over conventional micelles of increasing their hydrophobic core space, thus increasing the solubilization and loading capacities for drugs (16).

D- $\alpha$ -tocopheryl polyethylene glycol 1000 succinate (TPGS) a water-soluble derivative of vitamin E that has recently attracted focus in the arena of drug formulation. Being an amphiphilic molecule that comprises a hydrophobic head and a hydrophilic tail, TPGS has been considered as a promising solubilizing candidate that could provide efficient drug entrapment and emulsification capacity for lipidic formulations (17). Recently, TPGS has been successfully used for developing micelles alone or blended with other biocompatible materials (18). Phospholipids (PL), natural components of the cell membrane, represent a familiar class of biocompatible molecules. PL conjugates have been extensively employed to enhance the drugs' permeability and biological activity (19, 20).

Therefore, this study aimed at investigating the potential of SAMMs based on TPGS and PL for enhancing the antifungal activity of FLZ. Box-Behnken experimental design was utilized for designing an optimized micellar system with reduced size. The optimized formula was then examined for the antifungal activity against *C. albicans* in immunocompromised mice.

## EXPERIMENTAL

### Materials

Fluconazole, D- $\alpha$ -tocopherol polyethylene glycol 1000 succinate (TPGS), L- $\alpha$ -phosphatidylcholine phospholipids (PL) were purchased from Sigma-Aldrich (USA). All other reagents and solvents were analytical grade.

### Design of experiment applying Box-Behnken design

Response surface design (Box-Behnken) was applied for the development of FLZ loaded SAMMs using Design-Expert software (12.0; Stat-Ease Inc., USA). Three independent numerical variables were investigated, namely PL amount ( $X_1$ , mg), TPGS amount ( $X_2$ , mg), and sonication time ( $X_3$ , min) for their impacts on the particle size as a response ( $Y$ ). Table I shows the levels of the investigated factors.

As per the design, 17 experimental trials were generated by the software, including five centre points. Table II displays the combination of the independent variable's levels in each experimental run and its mean determined particle size. The optimal fitting sequential model was chosen by the model fit statistical analysis. The selection was performed based on the greatest adjusted and predicted  $R^2$  and the least predicted residual sum of squares (PRESS). 2D- contour and 3D- surface plots were developed to present the influence of the variables and the interaction between them.

### Preparation of FLZ loaded SAMMs

Solvent evaporation followed by film hydration was utilized for preparing FLZ loaded SAMMs (21, 22). Specified quantities of FLZ (50 mg), PL, and TPGS were dissolved in 50 mL ethanol. The solvent was then completely eliminated by rotary evaporation at reduced pressure at 45 °C for 45 min. The precipitated thin film was dispersed in 10 mL double distilled water and left for equilibration at ambient temperature for 2 h. The solution was magnetically stirred (1000 rpm) at a controlled temperature for 2 h and then sonicated at amplitude 40 %, 20 kHz, 750 W for the predefined time (Sonics Vibra Cell, Sonics & Materials Inc., USA). The resulting micellar dispersion was dialyzed to remove any un-trapped FLZ using a cellulose dialysis membrane tube (cut-off 12,000–14,000).

### Particle size determination of FLZ loaded SAMMs

Particle size (z-average) of FLZ loaded SAMMs in distilled water with proper dilution was measured using Zetatrac (Microtrac Inc., USA). Each measurement was repeated five times, and the particle size was displayed as the mean.

### Optimization of FLZ loaded SAMMs

The numerical approach integrating the desirability function was utilized for the optimization of FLZ loaded SAMMs. The optimized levels of the studied independent

Table I. Levels of formulation variables and particle size constraints used in the Box-Behnken design for the formulation of fluconazole loaded self-assembled mixed micelles

Independent variables	Levels		
	(-1)	(0)	(+1)
$X_1$ : PL amount (mg)	50	100	150
$X_2$ : TPGS amount (mg)	10	30	50
$X_3$ : Sonication time (min)	1	3	5
Responses	Desirability constraints		
$Y_1$ : Particle size (nm)	Minimize		

Table II. Combinations of variables' levels and observed particle size for fluconazole loaded self-assembled mixed micelles experimental runs

Experimental run	Independent variables			Particle size <sup>a</sup> ± SD (nm)
	PL amount (mg)	TPGS amount (mg)	Sonication time (min)	
F1	100	30	3	124 ± 3.1
F2	100	10	5	76 ± 1.9
F3	100	30	3	131 ± 5.2
F4	100	30	3	129 ± 4.8
F5	50	10	3	98 ± 2.8
F6	100	50	5	113 ± 3.6
F7	100	30	3	107 ± 3.1
F8	150	50	3	207 ± 5.5
F9	100	50	1	198 ± 4.2
F10	100	30	3	123 ± 2.8
F11	50	30	1	143 ± 3.3
F12	50	50	3	107 ± 2.9
F13	150	30	1	189 ± 4.1
F14	150	10	3	99 ± 2.4
F15	100	10	1	98 ± 2.6
F16	150	30	5	159 ± 3.9
F17	50	30	5	91 ± 2.1

<sup>a</sup> Mean ± SD, *n* = 5.

variables were anticipated based on the goals of decreasing particle size. The optimized formulation was then prepared for investigation of the antifungal activity.

### Characterization of the optimized formulation

Entrapment efficiency was calculated after quantifying the amount of incorporated drug, using the ultracentrifugation technique (23). To separate the un-entrapped drug, the specified volume of the optimized formulation was subjected to ultracentrifugation at 20,000 rpm at 4 °C for 30 min using cooling ultracentrifuge (Sigma 3–30 KS, Sigma Laborzentrifugen GmbH, Germany). The concentration of free drug in the supernatant was measured using a previously reported modified HPLC method, where the drug was determined at 211 nm (24).

*In vitro* release of FLZ from the optimized SAMMs formulation and LLZ gel were evaluated by the dialysis bag technique (25). FLZ loaded SAMMs dispersion and FLZ gel equivalent to 5 mg of FLZ was placed in cellulose dialysis bags having a molecular weight cut off from 12,000 to 14,000 Da. The bags were immersed in 50 mL phosphate buffer pH 5.5 and ethanol. The flask was kept in an incubator at 32 °C and stirred at 50 rpm. The specific volume of the samples was withdrawn at regular intervals over a period of 24 h and an equivalent volume of fresh buffer was added to the release medium to replenish it.

The release of FLZ from micelles and gel was determined using a previously reported modified HPLC method, where the drug was determined at 211 nm (31). The release study was performed in triplicate.

The viscosity of prepared FLZ-SLNs gels was measured using Brookfield viscometer (DV-II Pro Viscometer, USA) using the CPE-42 spindle.

#### *Antifungal activity assessment of optimized FLZ loaded SAMMs*

*Animals.* – Male Adults (Swiss mice) weighing 25–30 g were used. The animal study procedure obtained approval from the Animal Ethical Committee of the Faculty of Pharmacy, King Abdulaziz University (Reference number: PH-127-41). All procedures were carried out as per the Declaration of Helsinki. Animals were allowed to adapt in naturally controlled enclosures for a minimum of two weeks in dark/light cycles of 12 h each at  $20 \pm 1$  °C and fed with were fed pelleted food and water ad libitum.

*Candida and culture conditions.* – *C. albicans* (ATCC 90028) was kept on Sabouraud's dextrose agar (SDA) plate at 35 °C for 48 h. 5 mL of sterile phosphate buffer saline (0.85 %) was used to suspend the colonies. The concentration was adjusted to get  $2 \times 10^7$  colony forming units mL<sup>-1</sup>.

*Animal preparation and cutaneous infection.* – Twenty adult Swiss mice were randomly distributed among four groups ( $n = 5$ ). Cyclophosphamide ( $100 \text{ mg kg}^{-1} \text{ day}^{-1}$ ) was injected into mice intraperitoneally for three days before fungal infection to induce immunocompromised animals (26). Induction of cutaneous candidiasis model was made following the procedure published by Maebashi *et al.* (27) with some modification. The back of the mice was shaved with an electronic shaver (area  $2 \times 2$  cm). After 48 hours, the skin was moderately abraded with sandpaper. One hundred microliters of *Candida* cell suspension ( $2 \times 10^7$  cells) were gently applied by a cotton-tipped swab onto the skin.

*Treatment and evaluation of infection.* – Mice were divided into three groups. Treatments were given once a day for 5 successive days, starting 24 hours after candida infection. Group-1 was the negative control with no infection and no treatment (control group), group-2 was the positive control receiving infection with no treatment (untreated group), group-3 was given FLZ topically as a gel formulated using hydroxypropyl methylcellulose 1.5 % at a dose of  $10 \text{ mg kg}^{-1} \text{ day}^{-1}$  (FLZ group), and group-4 received an equivalent dose of FLZ-loaded SAMMs applied topically (FLZ loaded SAMMs group).

The infection was macroscopically evaluated by measuring erythema score from 0 to 4 as described: 0 – not erythematous (normal), 1 – mild erythema, 2 – moderate erythema, 3 – sparingly erythema and 4 – severe erythema (27).

To evaluate infection microbiologically, mice were sacrificed 24 hours following the last dose and  $1 \times 1$  cm of skin from the infected site was removed. This was then washed with sterile PBS, plated onto SDA plates and incubated at  $37 \pm 1$  °C for 48 hours. The colony-forming units (CFU) values of *C. albicans* were noted.

#### *Statistical analysis*

Data were statistically analyzed using one-way ANOVA and recorded as mean  $\pm$  SD using SPSS software (SPSS Inc., USA). GraphPad Prism 6 (GraphPad Software, USA) was used to estimate the confidence level (\*  $p < 0.01$  and \*\*  $p < 0.001$ ).

## RESULTS AND DISCUSSION

### *Fit statistics and diagnostic analysis*

The summary of fit statistics for particle size is displayed in Table III. Among the investigated polynomial models (linear, two-factor interaction, and quadratic), the best fitting model for the particle size of FLZ loaded SAMMs was the quadratic model as evidenced by its highest  $R^2$  and lowest PRESS. The adjusted  $R^2$  was in harmony with the predicted  $R^2$ . In addition, the adequate precision value was 19.85 which is greater than the desired value indicating an appropriate signal to noise ratio. Thus, the selected model could be considered adequate to navigate the experimental design space.

Diagnostic plots for particle size, developed for establishing the goodness of fit of the chosen model, are displayed in Fig. 1. Fig. 1a representing the Box-Cox plot for power transforms displays a recommended lambda ( $\lambda$ ) value of 1.97. The 95 % confidence interval (shown by the red lines) comprise the current  $\lambda$  value of 1; thereof no specific transformation for observed size is suggested (28). The un-necessity for transformation is advocated by the computed maximum to minimum particle size ratio of 2.72, where a ratio exceeding 10 probably calls for a transformation requirement. Studentized residual is a good criterion for identifying potential outliers that could influence the regression model. It could be computed by dividing the deleted residual by its estimated standard deviation. Fig. 1b represents a plot of the externally studentized residuals *vs.* predicted response values. This plot tests the assumption of constant variance; random distribution of the points in the plot within the limits implies the absence of constant error. Moreover, the residual *vs.* run plots, Fig. 1c, shows that no lurking variable could influence the measured size as evidenced by random scatter of points and absence of trends that could possibly indicate a time-related variable lurking in the background. The predicted *versus* observed size plot, Fig. 1d, was plotted to detect a value, or group of values, that are not easily predicted by the model; the plot reveals a highly linear correlation that reflects the harmony between the observed and predicted values indicating the suitability of the model (29).

### *Variables influence on particle size (Y)*

Nanoparticulate systems have shown good ability to circumvent the stratum corneum barrier, and consequently the reduced uptake rates of drugs upon topical treatment of skin disorders (30). Accordingly, the size is considered a crucial parameter for optimizing the proposed micelles. FLZ loaded SAMMs showed nanometric sizes ranging from  $76 \pm 1.9$  to

Table III. Fit summary statistics for the particle size of fluconazole loaded self-assembled mixed micelles

Source	SD	Sequential <i>p</i> -value	Lack of fit <i>p</i> -value	$R^2$	Adjusted $R^2$	Predicted $R^2$	PRESS
Linear	20.75	0.0002	0.0432	0.7659	0.7118	0.5319	11190.42
2FI	14.26	0.0143	0.1443	0.9149	0.8639	0.6544	8262.33
Quadratic	8.50	0.0161	0.6704	0.9788	0.9516	0.8768	2945.50

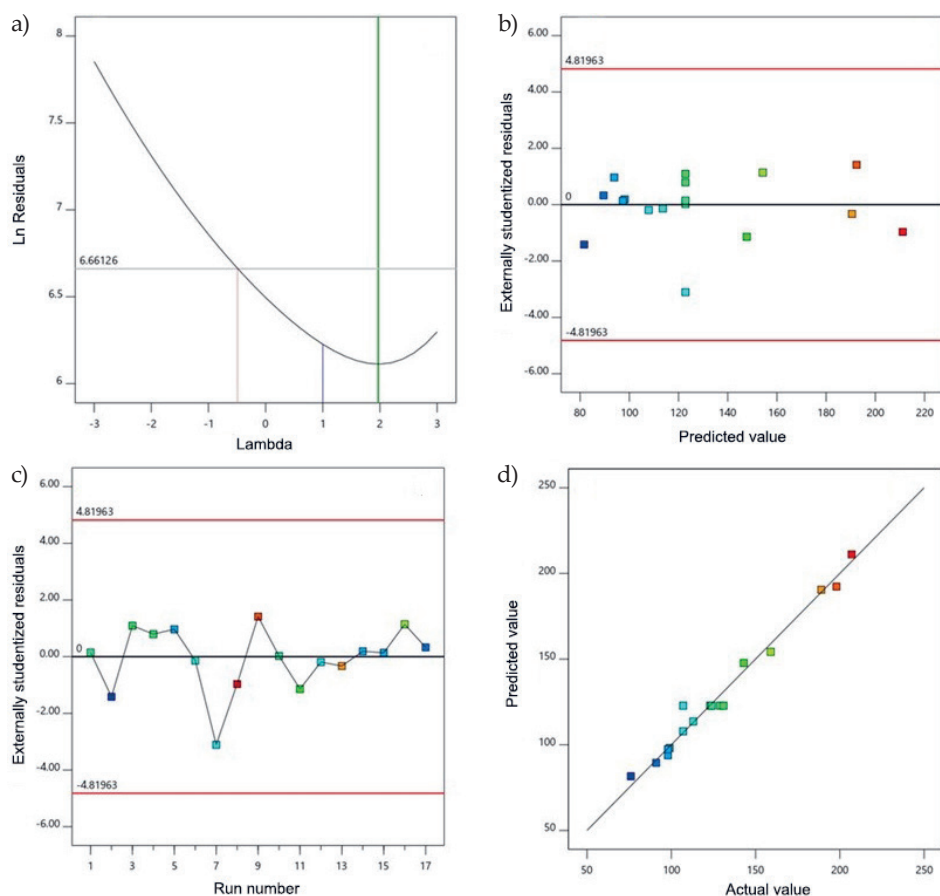


Fig. 1. Diagnostic plots for particle size of FLZ loaded SSAMMs: a) Box-Cox plot for power transforms, b) externally studentized residuals *vs.* predicted values plot, c) externally studentized residuals *vs.* run number plot, d) predicted *vs.* actual values plot.

198 ± 4.2 nm (Table II). Analysis of variance (ANOVA) according to the selected quadratic model revealed an F-value of 35.96 ( $p < 0.0001$ ). In terms of coded factor, the quadratic model equation for the particle size was generated as follows:

$$Y = 122.80 + 26.88X_1 + 31.75X_2 - 23.63X_3 + 24.75X_1X_2 + 5.50X_1X_3 - 15.75X_2X_3 + 14.60X_1^2 - 9.65X_2^2 + 8.10X_3^2$$

All linear terms ( $X_1$ ,  $X_2$ , and  $X_3$ ) referring to the three investigated variables displayed a significant impact on particle size ( $p = 0.0001$ ). The interaction terms between TPGS amount and either PL amount ( $X_1X_2$ ) or sonication time ( $X_2X_3$ ) were also significant ( $p = 0.0006$  and  $0.0076$ , respectively). Furthermore, the quadratic term  $X_1^2$  corresponding to the



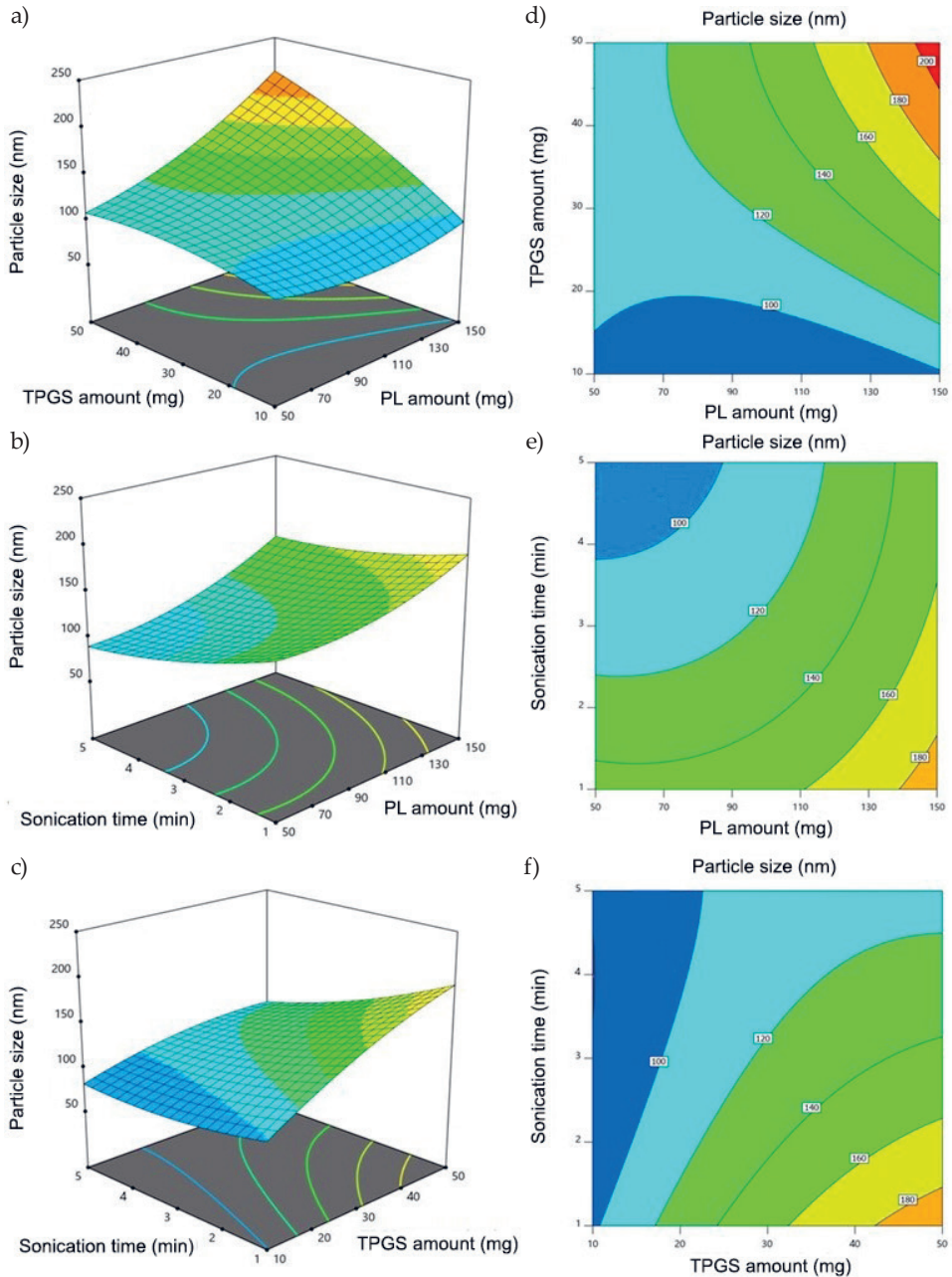


Fig. 2. a-c) 2D-contour plots and d-f) 3D-surface plots for the influence and interactions of PL amount ( $X_1$ ), TPGS amount ( $X_2$ ), and sonication time ( $X_3$ ) on the particle size of FLZ loaded SAMMs.



PL amount was also significant ( $p = 0.0097$ ). Fig. 2 illustrates the 2D-contour plots and 3D- for the effects and the interactions of the investigated variables on particle size.

It can be seen that the particle size increases with increasing PL and TPGS amounts while decreasing with increasing sonication time. Although surfactants are previously reported to reduce size in other studies, increasing TPGS resulted in higher particle sizes. Being a hydrophobic drug, FLZ tends to stay in the lipophilic phase; however, with an increase in surfactant concentration in the mixture, the drug might be diffused out from the hydrophobic core and solubilized in the external hydrophilic phase. More solubilization of FLZ outside the core might cause a reduction in the surfactant availability in the aqueous/organic interface and thus agglomeration of nano micelles may take place (31).

### Optimization

The numerical optimization method was selected according to the constraints previously set to particle size; the optimized levels of the investigated variables were anticipated as follows: 51.39 mg for PL amount, 49.75 mg for TPGS amount, and 4.94 min for sonication time. The particle size of the optimized formulation was evaluated following preparation. The percentage error (2.99 %) between the predicted (73.15 nm) and obtained particle size (75.34) was relatively small ensuring the appropriateness of the optimization process.

### Characterization of optimized SAMMs

The entrapment efficiency of FZL within the optimized FZL loaded SAMMs was found to be  $89.14 \pm 2.95$  %, which indicates that, the entrapment of FZL is high enough due to the entrapment of the drug within the hydrophobic core of the micellar structure. This effect can be connected to the solubility augmentation property of TPGS due to its amphiphilic nature as a result of the polar hydrophobic long carbon chain. This result is in agreement with the previously reported studies (22).

Since viscosity is an important parameter for characterizing the gels as it affects the extrudability, spreadability as well as the release of the drug. The viscosity of the optimized formulation was found to be 21000 cps. Easy spreadability is one of the important characteristics of topical gel formulations.

*In vitro* drug release from the optimized FLZ loaded SAMMs and FLZ gel were performed in PBS (pH 5.5 at 32 °C) using dialysis bag technique over 12 h and the cumulative release percentages are illustrated in Fig. 3. Data of the release profiles show that optimized FLZ-loaded SAMMs were capable to release FLZ in a controlled pattern over 24 h. The release profile achieved about 86 % drug release at the end of the period. It was found FLZ loaded SAMMs significantly improved the cumulative amount of permeated drug as compared with the raw FLZ gel. The higher release from the optimized formulation could be attributed to the enhanced solubility of the drug. The controlled pattern of release could be attributed to the PL component of the micelles, while the presence of TPGS could assist in enhancing the total amount released from the micelles. TPGS represents the hydrophilic portion in the mixed micelles that could facilitate the entry of water into the core of micelles forming hydrophilic channels (32). Thus, the proposed micellar formulation could enhance the solubility of FLZ while sustaining its release. The result obtained was in good agreement with previous studies (33).

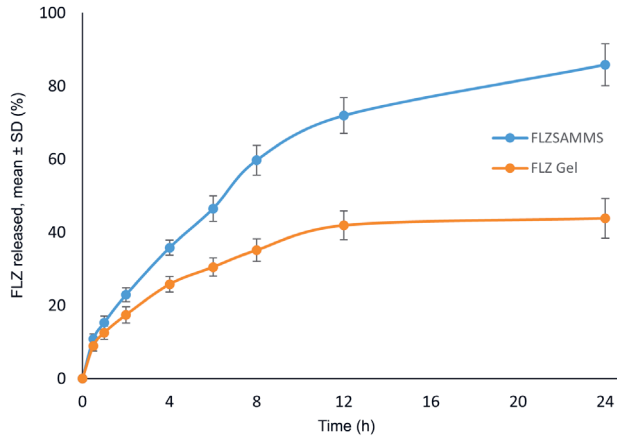


Fig. 3. *In vitro* release of optimized FLZ loaded SAMMs in phosphate buffer pH 5.5 at  $32 \pm 0.5$  °C.

### In vivo antifungal activity

Antifungal efficacy of FLZ loaded SAMMs was assessed in the treatment of candidiasis in immunocompromised mice models compared to FLZ gel. It is worthy to note that our aim was to compare the performance of our formulation with the standard drug solution. Since the formulation was intended for topical delivery, the drug solution was incorporated in a gel. A culture study was performed after 24 hours following the last dose on the 5<sup>th</sup> day of treatment. Skin samples taken after 24 h following the last dose were evaluated. The colony-forming units (CFU) of *C. albicans* in infected skin of mice after treatment are given in Table IV. From the results of the untreated group, it was clear that the number of pathogens was remarkably higher after 5 days of post-infection. The CFU were significantly reduced ( $*p < 0.01$ ) in the group treated with FLZ loaded SAMMs. Based on these results, it can be inferred that FLZ loaded SAMMs are effective in reducing the CFU as compared to FLZ gel in the treatment of candidiasis in immunocompromised mice.

The reduction in the CFU value of FLZ SAMMs might be attributed to the capability of the drug-loaded micelles to infiltrate through surrounding medium and fungal spores

Table IV. Colony-forming units (CFU) of *C. albicans* in the skin of mice after treatment with fluconazole (FLZ) loaded self-assembled mixed micelles (SAMMs) compared to fluconazole gel

Sample	Groups	Log CFU infected site
1	Control	0
2	Untreated	$14 \pm 2.2$
3	FLZ gel	$4.2 \pm 0.3$
4	FLZ loaded SAMMs	$1.2 \pm 0.01^a$

<sup>a</sup> Significant reduction in the fungal count of FLZ loaded SAMMs vs. FLZ treatment ( $p < 0.01$ ). Values represent mean  $\pm$  SD ( $n = 5$ ).

(34, 35). Moreover, the controlled release of FLZ resulted in a higher amount of drug at the site of infection for a longer period, and thus a reduction in fungal load was achieved as compared to FLZ gel. The reason for this might be the smaller size of micelles, and its enhanced solubility due to the presence of PLs and TPGS. This might be enabled a homogenous aqueous dispersibility which in turn increased the contact time of the drug with the spores and cells resulting in a possible rapid internalization of the drug (34).

Macroscopic evaluation of infection was assessed by the degree of erythema as an indication of skin irritation. A score of erythema from 0 to 4 was noted for the control group, untreated group, FLZ gel group and FLZ-SAMMs group (Fig. 4a). The erythema score was noted on day 1, day 3 and day 5 since the dosing was performed once a day for five consecutive days. It was found that there was a significant reduction in erythema score for the FLZ loaded SAMMs group on the 5<sup>th</sup> day of post-infection treatment. The FLZ loaded SAMMs treated group showed a score less than 1 while the untreated and FLZ treated group scored above 3. Thus, according to the results, it can be concluded that the developed optimized formulation not only reduced the irritation caused by the fungal infection but also proved that the formulation is non-irritant to the skin. So, the formulation can be considered as a non-irritant platform for application at the site of infection. This could be credited to the solubilization and entrapment of FLZ in the SAMMs. This contributes to a slow and continuous release of drug directly to the site of application with decreased wasting of the drug by migration to undesired areas (10).

Average lesion score in *C. albicans* induced candidiasis induced mice was noted for the control group, untreated group, FLZ gel group and FLZ loaded SAMMs group on day 5 post-infection (Fig. 4b). Lesion scores after inoculation of *C. albicans* in untreated as well as FLZ group were much higher than FLZ loaded SAMMs group. In all the groups, post-infection inflammation occurred and slightly erythematous lesions were observed initially and started to decrease with the treatment. It was found that in the FLZ loaded SAMMs group, the lesions were slowly relapsed and hardened with successive scaling. At end of the 5<sup>th</sup> day, it was found that treatment with the optimized formulation could clear the candidiasis

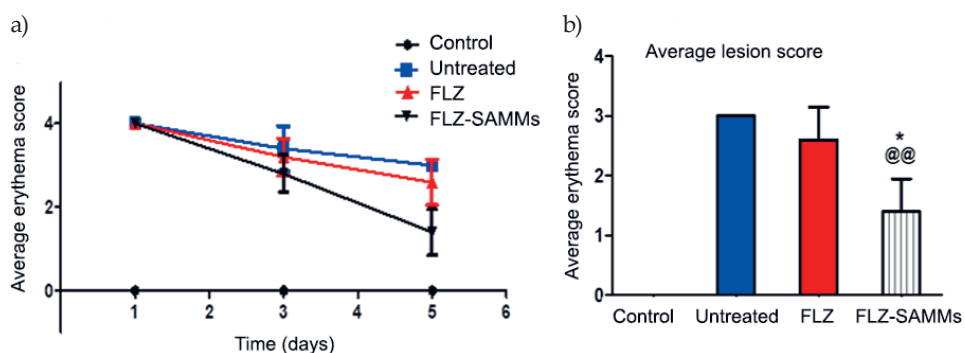


Fig. 4. Establishment of infection expressed as lesion scores after starting treatment in the cutaneous candidiasis mouse model. Mice (male adult,  $n = 5$ ) received  $10 \text{ mg}^{-1} \text{ kg}^{-1} \text{ day}^{-1}$  of fluconazole gel (FLZ group) or fluconazole-loaded SAMMs (FLZ-SAMMs group) applied topically for 5 days. a) Erythema scores were measured at days 1, 3 and 5, b) average lesion score on day 5. Data are presented as mean ( $n = 5$ ). @@ Significant FLZ-SAMMs vs. untreated ( $p < 0.0001$ ). \* Significant FLZ-SAMMs vs. FLZ ( $p < 0.001$ ).

infection even though the mice were immunocompromised (27). Therefore, it was concluded that the treatment with the optimized formulation led to decreased peripheral erythema as well as lesions associated with a fungal infection, in comparison to FLZ gel.

## CONCLUSIONS

Box-Behnken design and numerical optimization approach were successfully employed for the anticipation of the optimized FLZ loaded SAMMs with minimized particle size. The optimized formulation with an average observed size of 75.34 nm showed a superior *in vivo* antifungal activity against *C. albicans* in the immunocompromised mice model. In summary, the developed FLZ loaded SAMMs offers a promising vehicle for the topical delivery and treatment of cutaneous candidiasis. This novel delivery system could be exploited for skin targeting since it offers great potentials in dermal delivery and treatment for different types of cutaneous infection.

*Acknowledgement.* – This project was funded by the Deanship of Scientific Research (DSR) at King Abdulaziz University, Jeddah, under grant no. (RG-4–166–41). The authors, therefore, acknowledge with thanks the DSR for technical and financial support.

*Conflicts of interests.* – The authors declare no conflict of interest.

*Funding.* – This project was funded by the Deanship of Scientific Research (DSR) at King Abdulaziz University, Jeddah, under grant no. (RG-4–166–41).

*Authors' contributions.* – Conceptualization, U.F.; methodology, U.F., S.H., and A.A.; software, S.B.; validation, N.A. and H.A.; formal analysis, A.Y. and M.Q.; investigation, U.F., A.S. and M.A.; resources, U.F.; data curation, O.A., A.S., and M.A.; writing – original draft preparation, S.B. and S.K.; writing – review and editing, N.A., S.B. and S.K.; supervision, O.A.; project administration, H.A.; funding acquisition, S.B. All authors have read and agreed to the published version of the manuscript.

*Abbreviations.* – 2FI – two-factor interaction, FLZ – fluconazole, PL – phospholipid, PRESS – predicted residual error sum of squares, SAMMs – self-assembled mixed micelles, TPGS – D- $\alpha$ -tocopherol polyethylene glycol 1000 succinate.

## REFERENCES

1. B. Healy and R. Barnes, Topical and oral treatments for fungal skin infections, *Prescriber* 17(7) (2006) 30–43; <https://doi.org/10.1002/psb.360>
2. R. Coppola, S. Zanframundo, M. V. Rinati, M. Carbotti, A. Graziano, G. Galati, L. De Florio and V. Panasiti, *Rhodotorula mucilaginosa* skin infection in a patient treated with sorafenib, *J. Eur. Acad. Dermatol. Venereol.* 29(5) (2015) 1028–1029; <https://doi.org/10.1111/jdv.12455>
3. E. Palese, M. Nudo, G. Zino, V. Devirgiliis, M. Carbotti, E. Cinelli, D. M. Rodio, A. Bressan, C. Prezioso, C. Ambrosi, D. Scribano, V. Pietropaolo, D. Fioriti and V. Panasiti, Cutaneous candidiasis caused by *Candida albicans* in a young non-immunosuppressed patient: an unusual presentation, *Int. J. Immunopathol. Pharmacol.* 32 (2018) 1–4; <https://doi.org/10.1177/2058738418781368>
4. S. Bhattacharya, S. Sae-Tia and B. C. Fries, *Candidiasis* and mechanisms of antifungal resistance, *Antibiotics* 9(6) (2020) Article ID 312 (19 pages); <https://doi.org/10.3390/antibiotics9060312>
5. M. V. Martin, The use of fluconazole and itraconazole in the treatment of *Candida albicans* infections: a review, *J. Antimicrob. Chemother.* 44(4) (1999) 429–437; <https://doi.org/10.1093/jac/44.4.429>
6. P. Suchil, F. Montero Gei, M. Robles, A. Perera-Ramirez, O. Welsh and O. Male, Once-weekly oral doses of fluconazole 150 mg in the treatment of tinea corporis/cruris and cutaneous candidiasis, *Clin. Exp. Dermatol.* 17(6) (1992) 397–401; <https://doi.org/10.1111/j.1365-2230.1992.tb00246.x>

7. B. Darwesh, H. M. Aldawsari and S. M. Badr-Eldin, Optimized chitosan/anion polyelectrolyte complex based inserts for vaginal delivery of fluconazole: In vitro/in vivo evaluation, *Pharmaceutics* 10(4) (2018) Article ID 227 (16 pages); <https://doi.org/10.3390/pharmaceutics10040227>
8. H. M. Ellaithy and K. M. F. El-Shaboury, The development of Cutina lipogels and gel microemulsion for topical administration of fluconazole, *AAPS PharmSciTech* 3 (2002) 77–85; <https://doi.org/10.1208/pt030435>
9. M. Gupta, S. Tiwari and S. P. Vyas, Influence of various lipid core on characteristics of SLNs designed for topical delivery of fluconazole against cutaneous candidiasis, *Pharm. Dev. Technol.* 18(3) (2013) 550–559; <https://doi.org/10.3109/10837450.2011.598161>
10. V. Prajapati, A. Jain, R. Jain, S. Sahu and D. V. Kohli, Treatment of cutaneous candidiasis through fluconazole encapsulated cubosomes, *Drug Deliv. Transl. Res.* 4 (2014) 400–408; <https://doi.org/10.1007/s13346-014-0202-2>
11. T. O. McDonald, M. Siccardi, D. Moss, N. Liptrott, M. Giardiello, S. Rannard and A. Owen, *The Application of Nanotechnology to Drug Delivery in Medicine*, in *Nanoengineering Global Approaches to Health and Safety Issues*, Elsevier 2015, pp. 173–223.
12. W. Weng, Q. Wang, C. Wei, M. Adu-Frimpong, E. Toreniyazov, H. Ji, J. Yu and X. Xu, Mixed micelles for enhanced oral bioavailability and hypolipidemic effect of liquiritin: preparation, *in vitro* and *in vivo* evaluation, *Drug Dev. Ind. Pharm.* 47(2) (2021) 308–318; <https://doi.org/10.1080/03639045.2021.1879839>
13. O. A. A. Ahmed, K. M. El-Say, B. M. Aljaeid, S. M. Badr-Eldin and T. A. Ahmed, Optimized vinpocetine-loaded vitamin E D- $\alpha$ -tocopherol polyethylene glycol 1000 succinate-alpha lipoic acid micelles as a potential transdermal drug delivery system: *in vitro* and *ex vivo* studies, *Int. J. Nanomedicine* 2018(14) 33–43; <https://doi.org/10.2147/IJN.S187470>
14. O. A. A. Ahmed and S. M. Badr-Eldin, *In situ* misemgel as a multifunctional dual-absorption platform for nasal delivery of raloxifene hydrochloride: formulation, characterization, and *in vivo* performance, *Int. J. Nanomedicine* 2018(13) 6325–6335; <https://doi.org/10.2147/IJN.S181587>
15. J. Sobczykński and B. Chudzik-Rząd, *Mixed Micelles as Drug Delivery Nanocarriers*, in *Design and Development of New Nanocarriers*, Elsevier 2018, pp. 331–364.
16. L. C. Chen, Y. C. Chen, C. Y. Su, W. P. Wong, M. T. Sheu and H. O. Ho, Development and Characterization of lecithin-based self-assembling mixed polymeric micellar (saMPMs) drug delivery systems for curcumin, *Sci. Rep.* 6 (2016) Article ID 37122 (11 pages); <https://doi.org/10.1038/srep37122>
17. L. Mu and S. S. Feng, PLGA/TPGS nanoparticles for controlled release of paclitaxel: effects of the emulsifier and drug loading ratio, *Pharm. Res.* 20 (2003) 1864–1872; <https://doi.org/10.1023/B:PHAM.0000003387.15428.42>
18. J. Song, H. Huang, Z. Xia, Y. Wei, N. Yao, L. Zhang, H. Yan, X. Jia and Z. Zhang, TPGS/phospholipids mixed micelles for delivery of icarisperone II to multidrug-resistant breast cancer, *Integr. Cancer Ther.* 15(3) (2016) 390–399; <https://doi.org/10.1177/1534735415596571>
19. M. L. Manca, C. Cencetti, P. Matricardi, I. Castangia, M. Zaru, O. D. Sales, A. Nacher, D. Valenti, A. M. Maccioni, A. M. Fadda and M. Manconi, Glycrosomes: Use of hydrogenated soy phosphatidylcholine mixture and its effect on vesicle features and diclofenac skin penetration, *Int. J. Pharm.* 511(1) (2016) 198–204; <https://doi.org/10.1016/j.ijpharm.2016.07.009>
20. M. J. Naguib, S. Salah, S. A. Abdel Halim and S. M. Badr-Eldin, Investigating the potential of utilizing glycrosomes as a novel vesicular platform for enhancing intranasal delivery of lacidipine, *Int. J. Pharm.* 582 (2020) Article ID 119302 (14 pages); <https://doi.org/10.1016/j.ijpharm.2020.119302>
21. R. Shen, J. Kim, M. Yao and T. A. Elbayoumi, Development and evaluation of vitamin E D- $\alpha$ -tocopheryl polyethylene glycol 1000 succinate-mixed polymeric phospholipid micelles of berberine as an anticancer nanopharmaceutical, *Int. J. Nanomedicine* 2016(11) 1687–1700; <https://doi.org/10.2147/IJN.S103332>
22. N. A. Alhakamy, O. A. Ahmed, U. A. Fahmy, H. Z. Asfour, A. F. Alghaith, W. A. Mahdi, S. Alshehri and S. Md, Development, Optimization and evaluation of 2-methoxy-estradiol loaded nanocarrier

- for prostate cancer, *Front. Pharmacol.* **12** (2021) Article ID 682337 (14 pages); <https://doi.org/10.3389/FPHAR.2021.682337>
23. W. H. Abd-Elsalam, S. A. El-Zahaby and A. M. Al-Mahallawi, Formulation and *in vivo* assessment of terconazole-loaded polymeric mixed micelles enriched with Cremophor EL as dual functioning mediator for augmenting physical stability and skin delivery, *Drug Deliv.* **25**(1) (2018) 484–492; <https://doi.org/10.1080/10717544.2018.1436098>
  24. P. Sadasivudu, N. Shastri and M. Sadanandam, Development and validation of RP-HPLC and UV methods of analysis for fluconazole in pharmaceutical solid dosage forms, *Int. J. ChemTech Res.* **1**(4) (2009) 1131–1136.
  25. S. El-Housiny, M. A. S. Eldeen, Y. A. El-Attar, H. A. Salem, D. Attia, E. R. Bendas and M. A. El-Nabarawi, Fluconazole-loaded solid lipid nanoparticles topical gel for treatment of pityriasis versicolor: formulation and clinical study, *Drug Deliv.* **25**(1) (2018) 78–90; <https://doi.org/10.1080/10717544.2017.1413444>
  26. I. Angulo, M. B. Jiménez-Díaz, J. F. García-Bustos, D. Gargallo, F. Gómez de las Heras, M. A. Muñoz-Fernández and M. Fresno, *Candida albicans* infection enhances immunosuppression induced by cyclophosphamide by selective priming of suppressive myeloid progenitors for NO production, *Cell. Immunol.* **218**(1–2) (2002) 46–58; [https://doi.org/10.1016/S0008-8749\(02\)00521-X](https://doi.org/10.1016/S0008-8749(02)00521-X)
  27. K. Maebashi, T. Itoyama, K. Uchida, N. Suegara and H. Yamaguchi, A novel model of cutaneous candidiasis produced in prednisolone-treated guinea-pigs, *J. Med. Vet. Mycol.* **32**(5) (1994) 349–359; <https://doi.org/10.1080/02681219480000471>
  28. S. M. Badr-Eldin, N. A. Alhakamy, U. A. Fahmy, O. A. A. Ahmed, H. Z. Asfour, A. A. Althagafi, H. M. Aldawsari, W. Y. Rizg, W. A. Mahdi, A. F. Alghaith, S. Alshehri, F. Caraci and G. Caruso, Cytotoxic and pro-apoptotic effects of a sub-toxic concentration of fluvastatin on OVCAR3 ovarian cancer cells after its optimized formulation to melittin nano-conjugates, *Front. Pharmacol.* **11** (2021) Article ID 642171 (12 pages); <https://doi.org/10.3389/fphar.2020.642171>
  29. U. A. Fahmy, S. M. Badr-Eldin, O. A. A. Ahmed, H. M. Aldawsari, S. Tima, H. Z. Asfour, M. W. Al-Rabia, A. A. Negm, M. H. Sultan, O. A. A. Madkhali and N. A. Alhakamy, Intranasal niosomal *in situ* gel as a promising approach for enhancing flibanserin bioavailability and brain delivery: In vitro optimization and ex vivo/in vivo evaluation, *Pharmaceutics* **12**(6) (2020) Article ID 485 (23 pages); <https://doi.org/10.3390/pharmaceutics12060485>
  30. Z. M. Adib, S. Ghanbarzadeh, M. Kouhsoltani, A. Y. Khosroshahi and H. Hamishehkar, The effect of particle size on the deposition of solid lipid nanoparticles in different skin layers: A histological study, *Adv. Pharm. Bull.* **6**(1) (2016) 31–36; <https://doi.org/10.15171/apb.2016.006>
  31. R. Sharma, S. Kamboj, G. Singh and V. Rana, Development of aprepitant loaded orally disintegrating films for enhanced pharmacokinetic performance, *Eur. J. Pharm. Sci.* **84** (2016) 55–69; <https://doi.org/10.1016/j.ejps.2016.01.006>
  32. J. Singh, P. Mittal, G. Vasant Bonde, G. Ajmal and B. Mishra, Design, optimization, characterization and in-vivo evaluation of Quercetin enveloped Soluplus®/P407 micelles in diabetes treatment, *Artif. Cells Nanomedicine Biotechnol.* **46**(sup3) (2018) S546–S555; <https://doi.org/10.1080/21691401.2018.1501379>
  33. A. E. S. F. Abou El Ela and M. M. El Khatib, Formulation and evaluation of new long acting metoprolol tartrate ophthalmic gels, *Saudi Pharm. J.* **22**(6) (2014) 555–563; <https://doi.org/10.1016/j.jsps.2014.03.003>
  34. A. A. Alhowyan, M. A. Altamimi, M. A. Kalam, A. A. Khan, M. Badran, Z. Binkhathlan, M. Alkholief and A. Alshamsan, Antifungal efficacy of Itraconazole loaded PLGA-nanoparticles stabilized by vitamin-E TPGS: In vitro and ex vivo studies, *J. Microbiol. Methods* **161** (2019) 87–95; <https://doi.org/10.1016/j.mimet.2019.01.020>
  35. L. Qiu, B. Hu, H. Chen, S. Li, Y. Hu, Y. Zheng and X. Wu, Antifungal efficacy of itraconazole-loaded TPGS-b-(PCL-ran-PGA) nanoparticles, *Int. J. Nanomedicine* **2015**(10) 1415–1423; <https://doi.org/10.2147/IJN.S71616>